UDC 539.4

Deep-Drawing Process Simulation for Tailor-Welded Blanks with an Elastic Blankholder

A. Brusilová,[1] A. Schrek,[2] P. Švec,[3] and Z. Gábrišová[4]

Slovak University of Technology in Bratislava, Bratislava, Slovakia

[1] alena.brusilova@stuba.sk

[2] alexander.schrek@stuba.sk

[3] pavol.svec@stuba.sk

[4] zuzana.gabrisova@stuba.sk

Application of tailor welded blanks is proved to be very effective in the current trend of body parts construction. However, their formability is limited to the differences of mechanical properties of individual tailor welded blanks parts. These differences result in non-constant material flow and a deflection of the weld line. This article is focused on the elimination of uneven material flow and weld line instability. The results have been obtained by means of laboratory measurements on the drawing tool as well as material simulation computed by LS-DYNA code. According to acquired results, it can be claimed that the blankholder force values and force distribution have a significant influence on the deep-drawing process of tailor welded blanks. The weld line direction in consideration of the blankholder area size has influence on the deflection value. The simulation provided a reliable prediction of tailor-welded blank formability.

Keywords: tailor welded blank, deep-drawing, elastic blankholder, simulation.

Introduction. The manufacturing of modern vehicles bodyworks is associated with increase demand for the using of new materials and technologies. These growing requirements are related to safety increasing and fuel requirements reducing which are associated with reducing of total weight. These requirements can be met in the carrying bodyworks construction by using of drawn parts made of tailor welded blanks (TWBs) [1–4]. The TWBs are semi-finished parts that usually consist of materials with different stress-strain properties, but they can be made of materials with different thicknesses or coatings too. The joining of individual parts in TWB is usually created by laser welding. Several grades of steel can be used in TWBs design which enables to achieve the different stress-strain characteristic in certain sections of the drawn parts [5–8].

The application of different materials brings possible complications during the forming when it proves the considerable influence of stress-strain characteristics differences of the individual parts of TWB what result in non-constant material flow and consequently a negative deflection of the weld line [2, 8]. The formability is one of the most important properties of TWBs and it is influenced by different stress and strain properties of particular sheets from the view of planar and normal anisotropy. Material differences of used materials affect significantly the drawing parameters and complicate achieving of required properties of the drawn part. One of the ways of elimination this negative effect is to choose a suitable blankholder system with optimal distribution of blankholder forces by using an elastic blankholder with an adjustable distribution of blankholder forces [8–11]. Within the framework of this study, the experimental blankholder system with an elastic blankholder and an adjustable distribution of blankholder forces was used. Finite element method (FEM) simulation is instrumental to the study of TWB formability whereby it is possible to determine the values and points of application of the blankholder forces [12–14]. The FEM simulation results carried out via the simulative LS-Dyna software are

presented in this article. These were utilized to minimize the weld line deflection for TWBs consisting of DP600 and BH220 steel sheets by optimization of blankholder force values and distributions.

Experimental Procedure. Simulated and experimental weld line deflection values for the deep-drawing process of rectangular parts with dimensions of 120×80×40 mm were derived and compared. The parts were deep-drawn from TWBs consisting of DP600 dual-phase steel and BH220 bake-hardening steel with the same thickness of 1.2 mm.

Stress-Strain Characteristics of TWB Materials. The stress-strain characteristics of DP600 and BH220 steels used in simulations were defined by the flow curves. These were determined by means of the static tensile tests and measured values were manual put in Dynafrom software to run the simulations. The values of planar anisotropy coefficients r for both experimental steels in polar coordinates are compared in Fig. 1. For DP600, the flow stress values ranged from $\sigma = 350$ MPa at strain $\varphi = 0.02$ to $\sigma = 1300$ MPa at $\varphi = 1.00$, while the work-hardening coefficient achieved the value $n = 0.216$. The respective values of BH220 ranged from $\sigma = 280$ MPa at $\varphi = 0.02$ to $\sigma = 680$ MPa at $\varphi = 1.00$, and the work-hardening coefficient was $n = 0.157$.

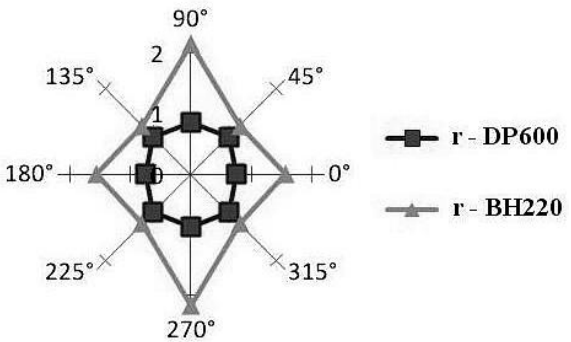

Fig. 1. Comparison of planar anisotropy coefficients r for steels DP600 and BH220.

Deep-Drawing Process Simulations. The TWB geometry with a thickness of 1.2 mm was determined by means of simulation via the Blank Size Engineering module of Dynaform software. Two variants of TWBs with the weld line oriented along the longitudinal and transversal direction of the axis of symmetry were used as seen in Fig 2.

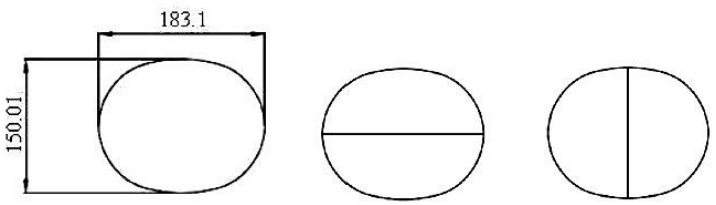

Fig. 2. TWB geometry and weld line orientations.

After surface mesh of TWBs, the nodal points of the weld line position on the TWBs were defined. The geometrical model of tool surfaces and blanks for a simple rectangular box drawing with dimensions 120×80×40 mm was constructed in CATIA V5 R19 software. Both simulations with uniform and non-uniform distribution of blankholder forces were evaluated. The blankholder material was chosen as the ideal elastic material model with a thickness of 35 mm and outer diameter of 190 mm, which deforms only elastically during real forming process. Four transfer pins with blankholder force measuring

elements, which contain tensometric gauges, were used to apply certain pressure on the blankholder. When the identical blankholder force value of 17 kN per each transfer pin with a circular area with diameter of 37 mm was applied, the uniform pressure (UNI mode) with the value of 7.8 MPa was achieved. Non-uniform pressure distribution (NON mode) was achieved when different balnkoholder force values were applied to the particular transfer pins and with higher value in the interval from 23 to 35 kN on the local transfer pin located at the BH220 steel sheet. It implies that 17 kN force per pin was applied to three pins and forces from 23 to 35 kN force were applied per each transfer pin. This higher force causes a local pressure increase from 7.7 MPa to 11.0 MPa. The bottom part of the deep-drawing tool with TWB pressed to the blankholder and with eight transfer pins is depicted in Fig. 3. The tool model for deep-drawing simulations is shown in Fig. 4. Eight circles represent the positions of transfer pins, four of which are used for applying the uniform or non-uniform blankholder forces and corresponded pressure distributions in Fig. 4.

Fig. 3. Part of deep-drawing tool with TWB.

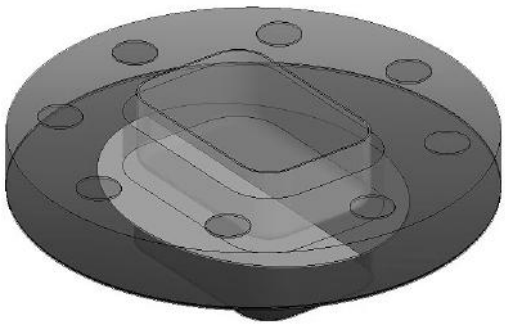

Fig. 4. Tool model for deep-drawing simulations.

Results and Discussion. The elastic deformation of the blankholder plate under uniform blankholder force distribution at deep-drawing of TWB with longitudinal weld line orientation is presented in Fig. 5. The bending deformation of the blankholder was symmetrical and more intensive in the transversal direction than in the longitudinal one. The elastic deformation of the blankholder plate for the non-uniform blankholder force distribution during deep-drawing of TWB with the longitudinal weld line orientation is illustrated in Fig. 6. The highest vertical deflection of 0.19 mm was observed in the contact area of the transfer pin with the blankholder surface as can be seen from the simulation in Fig. 6. The local blankholder force applied on this transfer pin was 35 kN, which was the highest experimental value.

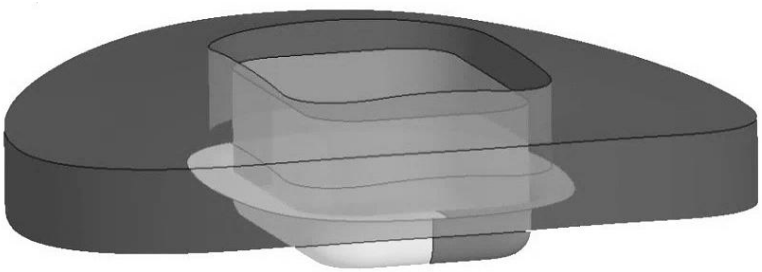

Fig. 5. Deformation of blankholder for uniform blankholder force distribution with 17 kN per pin.

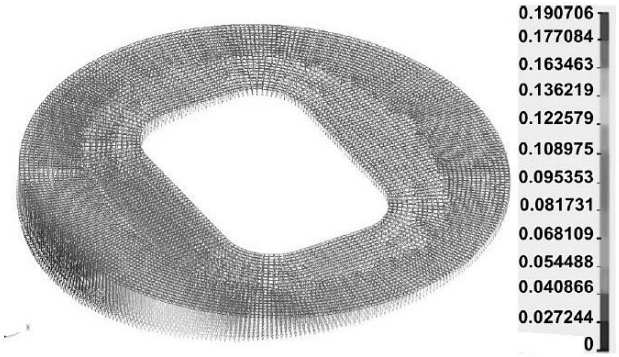

Fig. 6. Deformation of blankholder for non-uniform blankholder force distribution with 35 kN on the local pin.

The LS-DYNA code was used to run the simulations. The blankholder forces in the interval from 17 to 35 kN were applied tot particular transfer pins to achieve various distributions of blankholder forces and pressures along the elastic blankholder circumference. The other parameters, such as blank area, blank thickness, speed of the punch, friction coefficient, tool geometry (punch and die corner radius, drawing gap), were constant. The distribution of stresses at two stages of simulation of deep-drawing process is illustrated in Fig. 7. The high effective stress above 1200 MPa was generated originated in the corners of rectangular drawn part in DP600 steel. As the normal anisotropy of this steel is lower than that of BH220 steel, the increase in the corner thickness (DP600 steel) is respectively higher, and, as a the consequence, the intensive compression of DP600 steel in both the area between blankholder and die and in the drawing gap is observed. As the material is only bent and straightened at narrow flat circumferential parts of drawn part, the stresses are considerably smaller (600 MPa), as compared to those in the corners of the drawn part (1200 MPa). Both TWBs with the longitudinal and transversal weld line orientations and a uniform adjustment of the blankholder pressure of 7.8 MPa showed a considerable deflection of the weld line towards the DP600 steel.

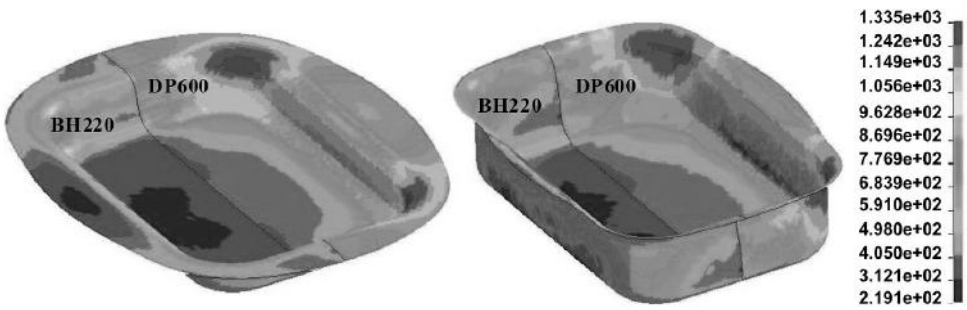

Fig. 7. Effective stress distribution during deep-drawing simulation of TWB with the longitudinal weld line orientation.

Contact pressure distribution during deep-drawing of TWB with longitudinal weld line orientation at uniform blankholder force distribution (17 kN on every transfer pins) is in Fig. 8. The pressure distribution at non-uniform blankholder force distribution (35 kN on local transfer pin applied on BH220 steel) is in Fig. 9. The pressure distribution of TWB with the transversal weld line orientation in cases of uniform and non-uniform blankholder force distributions is shown in Figs. 10 and 11, respectively. The force value transferred by

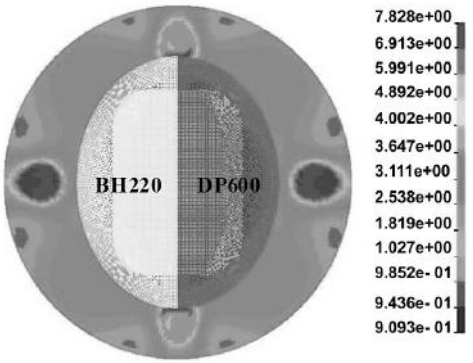

Fig. 8

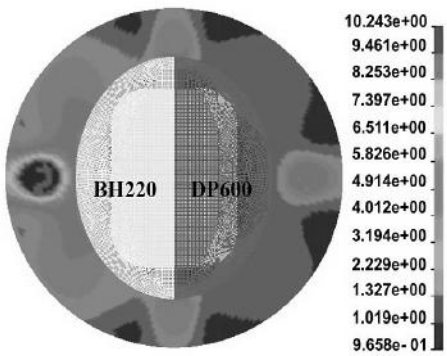

Fig. 9

Fig. 8. Pressure distribution for uniform blankholder force distribution with 17 kN per pin.
Fig. 9. Pressure distribution for non-uniform blankholder force distribution with 35 kN on the local pin.

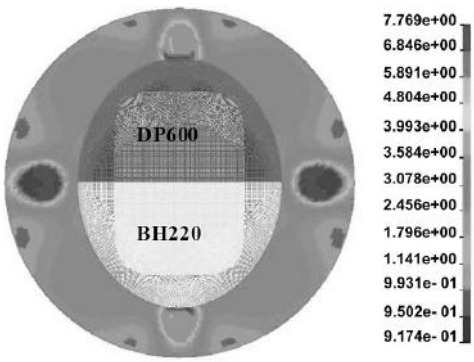

Fig. 10

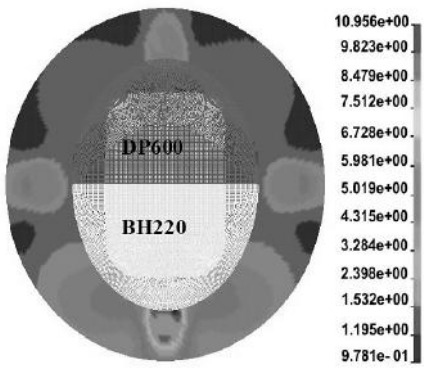

Fig. 11

Fig. 10. Pressure distribution at uniform blankholder force distribution with 17 kN per pin.
Fig. 11. Pressure distribution at non-uniform blankholder force distribution with 35 kN on the local pin.

local pin had to be increased up to 35 kN in these simulations (Figs. 9 and 11) to achieve the smallest deflection of the weld line. The application of a higher force to the BH220 steel sheet (yellow area in Fig. 9 and 11) provided the minimization of the weld line deflection. The local increase in the contact pressure can be observed when comparing Fig. 8 with Fig. 9 and Fig. 10 with Fig. 11.

The Nodal Displacement Measurements. The deflections of the weld lines for TWBs produced from DP600 and BH220 steels were evaluated in the perpendicular directions to the weld lines, and the results are presented for two different weld line orientations in Figs. 12 and 13, respectively. The DP600 steel is depicted in darker colors and the BH220 steel in brighter ones in Figs. 12 and 13. The simulations in both figures show the nodal displacements of the points in the TWB center in different axial directions. The displacements determined by LS-Pre-Post in History code of the simulation software are marked by arrows in Figs. 12 and 13. The uniform blankholder force distribution with the force of 17 kN per each transfer pin caused a significant deflection of the weld line (marked by UNI-17 kN) in Figs. 12 and 13. The non-uniform blankholder force distribution allows one to reduce the weld deflection by increasing the local blankholder force in the interval from 23 to 35 kN. The weld line deflection was hampered by excessively strong holding of flange on the more ductile BH220 steel sheet. The optimal blankholder force values for the

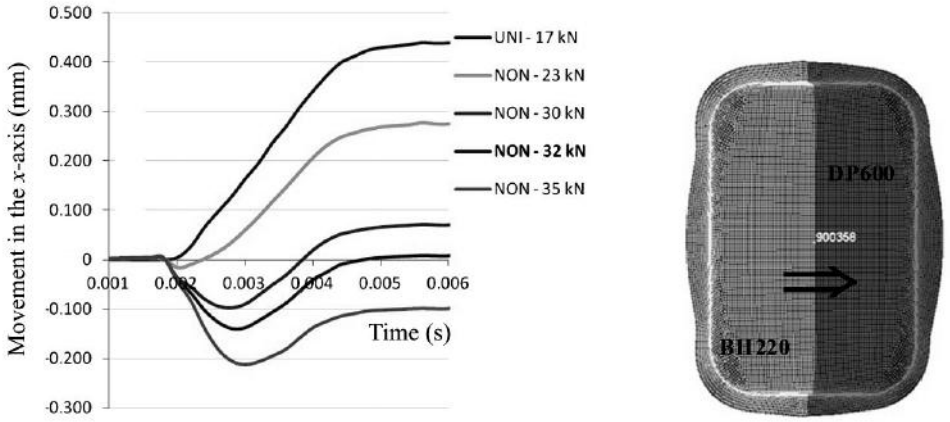

Fig. 12. Simulation of weld line deflection represented by the nodal displacements of points in the TWB center in the *x*-axis direction for the uniform blankholder force distribution and longitudinal weld line orientation.

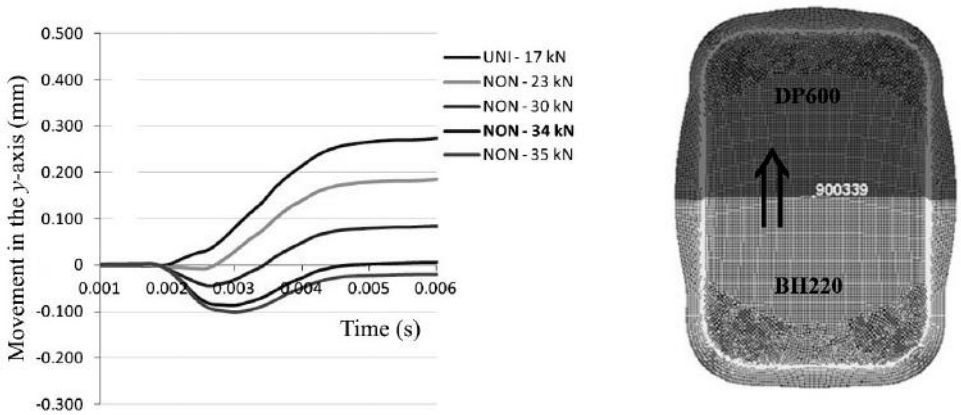

Fig. 13. Simulation of weld line deflection represented by nodal displacements of points in the TWB center in the *y*-axis direction for the uniform blankholder force distribution and transversal weld line orientation.

non-uniform blankholder force distribution, which ensured the minimal weld line deflection and the weld line comeback to the initial central position at the end of the forming process, corresponds to the local force of 32 kN (Fig. 12) and 34 kN (Fig. 13) for *x*- and *y*-axes, respectively. This implies that a slightly higher (by 2 kN) local force is needed to minimize the weld line deflection for the transversal weld line orientation, as compared to the longitudinal one.

The Comparison of Simulated and Experimental Weld Line Positions. The weld line deflection observed on the walls of the drawn part obtained via simulations and experiments were compared visually by means of overlaying the experiemental photos of the drawn part walls with the FEM mesh of simulated drawn parts. The side wall of drawn part with the longitudinal welded TWB with deformed weld line for the uniform distribution of blankholder forces is shown in Fig. 14. The overlay image in Fig. 15 shows a good fit of simulated and experimental weld lines. The wall of drawn cup area shows the deformation of material in the die holding area where stronger and less ductile material (DP600 steel) pushes a less strong and more ductile material (BH220 steel).

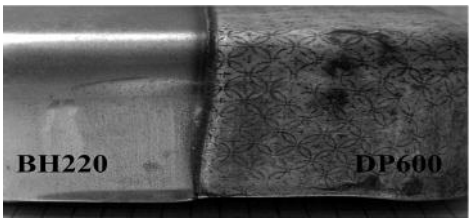

Fig. 14

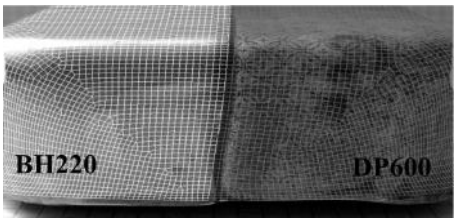

Fig. 15

Fig. 14. Experimental weld line deflection with the longitudinal orientation of the weld line.
Fig. 15. Simulated weld line deflection with the longitudinal orientation of the weld line.

Fig. 16

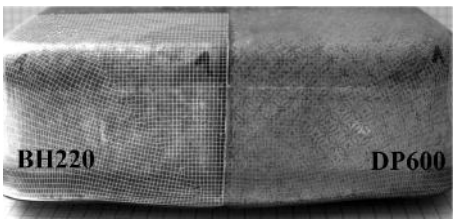

Fig. 17

Fig. 16. Experimental weld line deflection for the transversal orientation of the weld line.
Fig. 17. Simulated weld line deflection for the transversal orientation of the weld line.

The side wall of drawn cup with the transversal orientation of the derformed weld line for the uniform blankholder force distribution mode is depicted in Fig. 16. The overlay image in Fig. 17 also shows a good fit of simulated and experimental weld lines. The deformation direction is the same as in the previous experiment. However, this deformation is smaller in comparison to the drawn cup with the longitudinal orientation of the weld line.

Conclusions. The deep-drawing of TWBs consisting of dual-phase DP600 and bake-hardening BH220 steels with a thickness of 1.2 mm was analyzed. The aim was to verify the effect of blankholder force distribution on the minimization of the weld line deflection. The elastic blankholder model was used for the simulations. Both simulated and experimental deep-drawing processes were realized for TWBs with the longitudinal and transversal orientations of the weld line. Two blankholder force distributions, namely, uniform and non-uniform ones, were monitored. The optimal distribution of blankholder forces for the weld line stabilization was identified.

The results obtained confirmed a good conformity of simulated and experimental results. The weld line deflection of TWB is a result of different stress-strain characteristics of the TWB materials. The weld line orientation is shown to strongly affect its deflection. The most intensive deflections of weld line were observed for the longitudinal orientation of the weld line. They were influenced by the lengths of narrow sections of drawing edges and the blankholder area sizes. The most intensive deflection of the weld line was observed on the walls of drawn parts. The blankholder force values and their distribution have a significant influence on the deep-drawing process of TWBs. A visual comparison of the weld line deflections revealed a good fit of simulated and experimental results, which proved the reliability of the proposed simulation method for the TWB formability predictions.

Acknowledgments. This work was supported by the Slovak Research and Development Agency under the contract No. APVV-0281-12.

1. V. V. N. Satya Suresh, S. P. Regalla, A. K. Gupta, and G. Padmanabham, "Weld line shift in the case of tailor welded blanks subjected to differential strengths with respect to TIG and laser welding," *Mater. Today - Proc.*, **2**, Nos. 4–5, 3501–3510 (2015).
2. B. Kinsey and X. Wu, *Tailor Welded Blanks for Advanced Manufacturing*, Woodhead Publishing, Cambridge (2011).
3. P. Švec, A. Schrek, and T. Csicsó, "Fiber laser welding of dual-phase and bake-hardened steels," *Strength Mater.*, **48**, No. 4, 481–486 (2016).
4. P. Bałon, A. Świątoniowski, and J. Szostak, "Improved method of springback compensation in metal forming analysis," *Strength Mater.*, **48**, No. 4, 540–550 (2016).
5. E. Evin and M. Tomáš, "Comparison of deformation properties of steel sheets for car body parts," *Procedia Engineer.*, **48**, 115–122 (2012).
6. J. Bílik, M. Balážová, L. Kršiaková, and R. Šuba, "The analyssis of properties and forming duplex steel DP 450," *Hutnicke Listy*, **63**, No. 4, 74–77 (2010).
7. W. Fracz, F. Stachowicz, T. Trzepiecinski, and T. Pieja, "Forming limit of the heat resistant AMS 5599 sheet metal," *Hutnik-WH*, **81**, No. 7, 442–445 (2014).
8. M. Merklein, M. Johannes, M. Lechner, and A. Kuppert, "A review on tailored blanks – Production, applications and evaluation," *J. Mater. Process. Tech.*, **214**, No. 2, 151–164 (2014).
9. J. Bílik, J. Ertel, J. Bárta, et al., "The analyssis of properties and forming of laser welded superduplex steel SAF 2507," *Hutnik-WH*, **82**, No. 9, 627–631 (2015).
10. Y. Morishita, T. Kado, S. Abe, et al., "Role of counterpunch for square-cup drawing of tailored blank composed of thick/thin sheets," *J. Mater. Process. Tech.*, **212**, 2102–2108 (2012).
11. L. Kaščák, E. Spišák, R. Kubik, and J. Mucha, "FEM analysis of clinching tool load in a joint of dual-phase steels," *Strength Mater.*, **48**, No. 4, 533–539 (2016).
12. Z. Q. Zhang, X. F. Jia, Y. J. Wang, and P. Gao, "Optimization analysis of initial sheet metal contour line for high-strength boron steel in hot stamping," *Strength Mater.*, **48**, No. 1, 77–81 (2016).
13. J. Slota, M. Jurčišin, and E. Spišák, "Experimental and numerical analysis of local mechanical properties of drawn part," *Key Eng. Mat.*, **586**, 245–248 (2014).
14. A. Khan, V. V. N. Satya Suresh, and S. P. Regalla, "Effect of thickness ratio on weld line displacement in deep-drawing of aluminium steel tailor welded blanks," *Proc. Mat. Sci.*, **6**, 401–408 (2014).

Received 01. 09. 2017